Supplementary Information

Boosting ppb-level tiethylamine sensing of ZnO: adjusting proportions of electron donor defects

Wenjing Wei[a#], Jingxiang Zhao[a#], Shaoxuan Shi[a#], Huiming Lin[a], Zhu Mao[b], Feng Zhang[a*] and Fengyu Qu[a*]

a. Key Laboratory of Photochemical Biomaterials and Energy Storage Materials, Heilongjiang Province and College of Chemistry and Chemical Engineering, Harbin Normal University, Harbin 150025, P. R. China

b. School of Chemistry and Life Science, Advanced Institute of Materials Science, Changchun University of Technology, Changchun 130012, China

# These authors contributed equally to this work

*Corresponding authors: Feng Zhang (E-mail: zhangfeng@hrbnu.edu.cn) and Fengyu Qu (E-mail: qufengyu@hrbnu.edu.cn)

Mott−Schottky (M-S) curves and electrochemical impedance spectroscopy (EIS): The ZnO, saturated calomel electrode (SCE) and Pt wire was used as working electrode, reference electrode and pair electrode, respectively, detected in 0.1 M Na_2SO_4. ZnO was evenly mixed with ethanol, and then the paste was dropped on tin fluoride oxide (FTO) glass (1.0×1.0 cm^2), and dried at 60 ℃. M-S curves were measured voltages of -0.6v to 0.6v versus SCE at frequencies of 100 Hz, 500 Hz, 1000 Hz at room temperature, respectively. EIS was carried out using a frequency range from 1000000 to 0.1 Hz at room temperature.

Theoretical model and calculations: The DMol^3 module was used to perform all spin-polarized DFT simulations[1], and the exchang-correlation interactions were treated using the Perdew-Burke-Ernzerhof (PBE) functional within a generalized gradient approximation (GGA)[2]. For the possible van der Waals interactions, the Grimme (DFT-D2) scheme was employed in all calculations[3]. For the involved Zn atoms in these catalysts, the density functional semi-core pseudopotential (DSPP) was adopted to treat their core electrons[4], whereas the double numerical plus polarization (DNP) basis set was employed for other elements. Self-consistent field (SCF) calculations were carried out with a convergence criterion of 10^{-6} a.u. on the total energy. The hybrid functionals based on the Heyd−Scuseria−Ernzerhof (HSE06) method[5] were adopted to get the exact band structures of the pristine and defective ZnO materials.

To simulate the O_2 adsorption, ZnO(100) was used, which has a four layer structure. The Brillioun zone was sampled using a 5 × 5 × 1 k-points for the geometry optimization The adsorption energy (E_{ads}) of O_2 molecule on substrate can be determined according to the following definition: $E_{ads} = E_{total}$(adsorbed systems) – E_{total}(adsorbate) – E_{total}(substrate), where E_{total}, represent the total energies for the systems in the bracket.

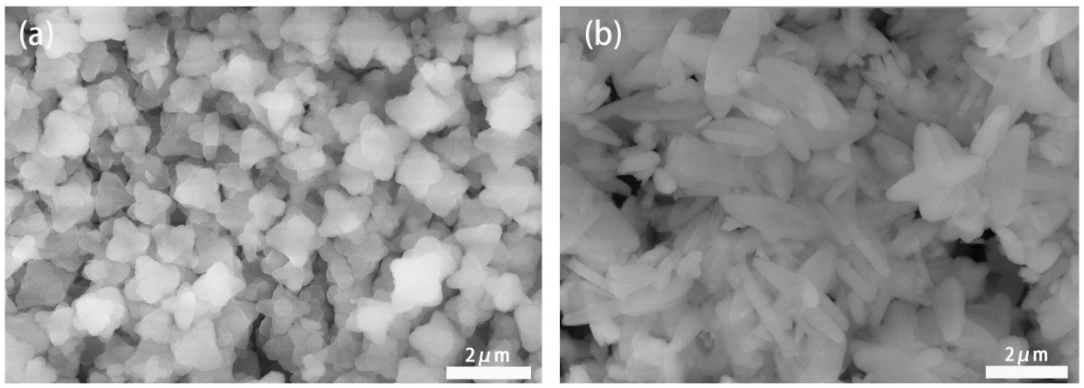

Fig. S1 SEM images of ZIF-II (a) and ZIF-IV (b)

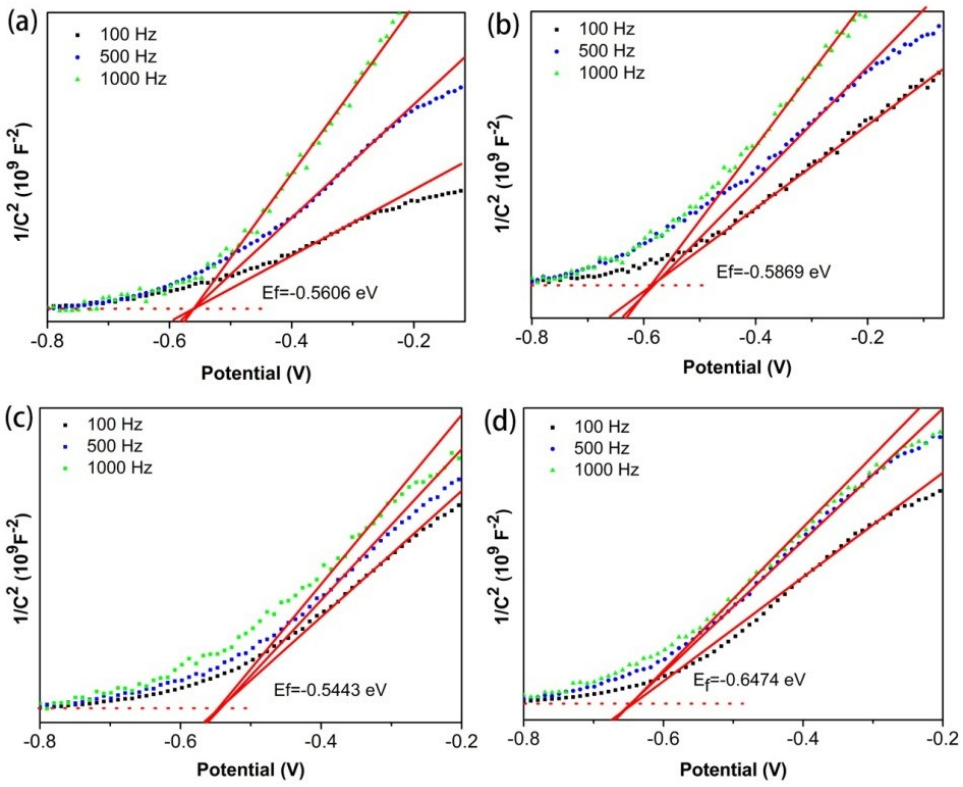

Fig. S2 Mott-Schotty plots of ZnO-X ((a) I, (b) II, (c) III and (d) IV) at 100 Hz, 500 Hz, 1000 Hz, respectively.

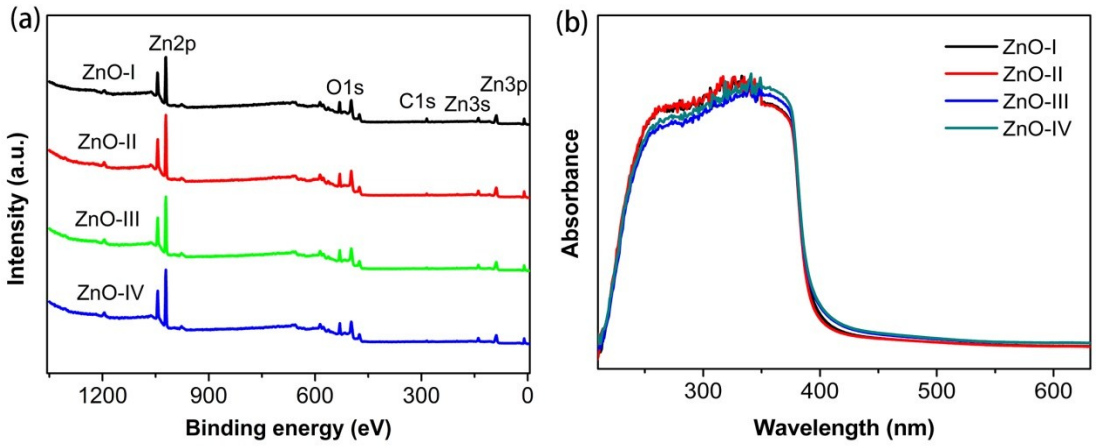

Fig. S3 (a) XPS survey and (b) UV-vis diffuse reflectance spectra of ZnO-X (I, II, III, IV).

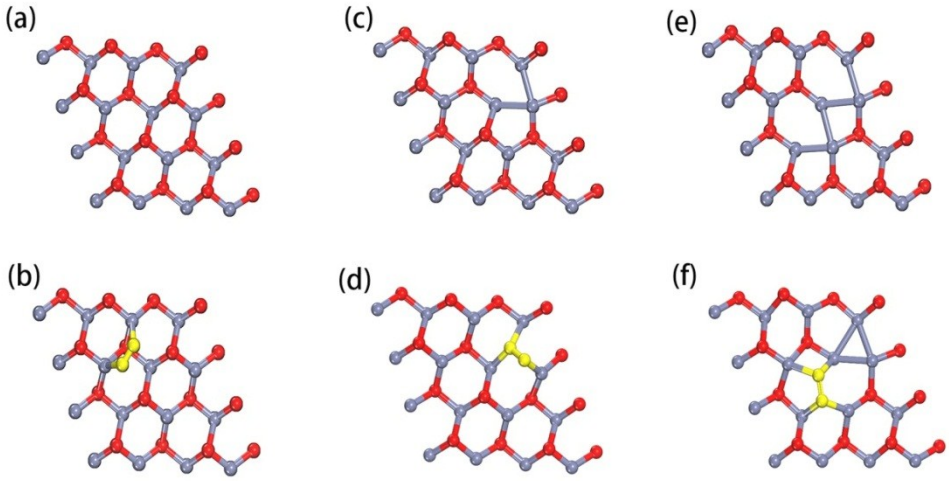

Fig. S4 The (100) surface of ZnO with 0% (a, b), 12.5% (c, d) and 25 % (e, f) oxygen vacancies before (a, c, e) and after (b, d, f) adsorption of oxygen. The red, blue and yellow balls represent O, N and adsorbed O atoms, respectively.

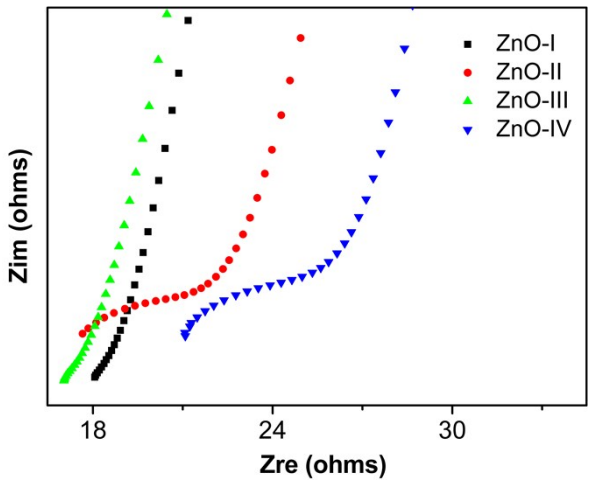

Fig. S5 Nyquist impedance plot of ZnOs (I, II, III and IV).

Table S1 The sensing performances of various materials based TEA sensors.

Material	Concentration (ppm)	Sensitivity	Operating temperature (ºC)	detection limit (ppm)	Ref.
Pd/In_2O_3	50	47.56	220	1	[6]
SnO_2/ZnO	50	17.7	200	10	[7]
WO_3 hollow microspheres	50	16	220	5	[8]
$ZnO/ZnCo_2O_4$	100	5.12	220	5	[9]
Zn_2SnO_4/ZnO	100	175.5	200	0.4	[10]
$Ag/SnO_2/rGO$	100	82.47	220	0.5	[11]
SnO_2 hollow microfiber	100	49.5	270	2	[12]
CuO particles	100	102	230	5	[13]
$Cr/\alpha\text{-}MoO_3$	100	150.25	200	1	[14]
ZnO	50 100	773 1133.5	275	0.2	This work

Table S2 The BET surface area, atomic proportion and band-gap width of ZnO-X.

	ZnO-I	ZnO-II	ZnO-III	ZnO-IV
BET surface area ($m^2\ g^{-1}$)	8.98	3.79	5.25	2.7685
O_S/O atomic (%)	26.03	22.43	28.44	24.39
band-gap width (eV)	3.178	3.190	3.161	3.195

Table S3 Related electrochemical parameters.

	ZnO-I	ZnO-II	ZnO-III	ZnO-IV
500 Hz N_D (cm^{-3})	5.7×10^{21}	5.4×10^{21}	5.8×10^{21}	3.3×10^{21}
E_{CB} (eV) vs SCE	-0.5606	-0.5869	-0.5443	-0.6474
E_{VB} (eV) vs SCE	-3.7386	-3.7769	-3.7053	-3.8424

Table S4 The relative intensity $I(E_1(LO)/I(E_2(high)$ of $E_1(LO)$ to $E_2(high)$ mode.

	ZnO-I	ZnO-II	ZnO-III	ZnO-IV
$I(E_1(LO))$	265.73	350.48	404.65	48.41
$I(E_2(high))$	1543.31	1557.86	1555.48	1223
$I(E_1(LO))/I(E_2(high))$	0.17	0.23	0.26	0.0396

Table S5 Theoretical calculation of relevant parameter.

	ZnO-I (0%)	ZnO-II (12.5%)	ZnO-III (25%)
Binding energy (eV)	0.14	1.70	2.39
Band-gap width (eV)	2.54	2.67	2.37

Reference

[1] a) B. Delley, *The Journal of Chemical Physics* **2000**, *113*, 7756-7764; b) B. Delley, *The Journal of Chemical Physics* **1990**, *92*, 508-517.

[2] J. P. Perdew, K. Burke and M. Ernzerhof, *Physical Review Letters* **1997**, *78*, 1396-1396.

[3] S. Grimme, *Journal of Computational Chemistry* **2006**, *27*, 1787-1799.

[4] B. Delley, *Physical Review B* **2002**, *66*, 155125.

[5] J. Heyd, G. E. Scuseria and M. Ernzerhof, *The Journal of Chemical Physics* **2003**, *118*, 8207-8215.

[6] X. Liu, K. Zhao, X. Sun, C. Zhang, X. Duan, P. Hou, G. Zhao, S. Zhang, H. Yang, R. Cao and X. Xu, *Sensors and Actuators B: Chemical* **2019**, *285*, 1-10.

[7] Q. Ma, S. Chu, Y. Liu, Y. Chen, J. Song, H. Li, J. Wang, Q. Che, G. Wang and Y. Fang, *Materials Letters* **2019**, *236*, 452-455.

[8] C. Zhai, M. Zhu, L. Jiang, T. Yang, Q. Zhao, Y. Luo and M. Zhang, *Applied Surface Science* **2019**, *463*, 1078-1084.

[9] Y. Li, N. Luo, G. Sun, B. Zhang, H. Jin, L. Lin, H. Bala, J. Cao, Z. Zhang and Y. Wang, *Sensors and Actuators B: Chemical* **2019**, *287*, 199-208.

[10] F. Liu, X. Chen, X. Wang, Y. Han, X. Song, J. Tian, X. He and H. Cui, *Sensors and Actuators B: Chemical* **2019**, *291*, 155-163.

[11] S. Zhang, B. Zhang, G. Sun, Y. Li, B. Zhang, Y. Wang, J. Cao and Z. Zhang, *Materials Research Bulletin* **2019**, *114*, 61-67.

[12] Y. Zou, S. Chen, J. Sun, J. Liu, Y. Che, X. Liu, J. Zhang and D. Yang, *ACS Sensors* **2017**, *2*, 897-902.

[13] Y.P. Wu, W. Zhou, W.W. Dong, J. Zhao, X.Q. Qiao, D.F. Hou, D.S. Li, Q. Zhang and P. Feng, *Crystal Growth & Design* **2017**, *17*, 2158-2165.

[14] W. Li, S. He, L. Feng and W. Yang, *Materials Letters* **2019**, *250*, 143-146.